



## Test of CPT and Lorentz symmetry in entangled neutral kaons with the KLOE experiment



KLOE-2 Collaboration

D. Babusci<sup>h</sup>, I. Balwierz-Pytko<sup>g</sup>, G. Bencivenni<sup>h</sup>, C. Bloise<sup>h</sup>, F. Bossi<sup>h</sup>, P. Branchini<sup>t</sup>, A. Budano<sup>s,t</sup>, L. Caldeira Balkestahl<sup>v</sup>, G. Capon<sup>h</sup>, F. Ceradini<sup>s,t</sup>, P. Ciambrone<sup>h</sup>, F. Curciarello<sup>i,d</sup>, E. Czerwiński<sup>g</sup>, E. Danè<sup>h</sup>, V. De Leo<sup>i,d</sup>, E. De Lucia<sup>h</sup>, G. De Robertis<sup>b</sup>, A. De Santis<sup>o,p,\*</sup>, P. De Simone<sup>h</sup>, A. Di Cicco<sup>s,t</sup>, A. Di Domenico<sup>o,p</sup>, C. Di Donato<sup>k,l</sup>, R. Di Salvo<sup>r</sup>, D. Domenici<sup>h</sup>, O. Erriquez<sup>a,b</sup>, G. Fanizzi<sup>a,b</sup>, A. Fantini<sup>q,r</sup>, G. Felici<sup>h</sup>, S. Fiore<sup>o,p</sup>, P. Franzini<sup>o,p</sup>, A. Gajos<sup>g</sup>, P. Gauzzi<sup>o,p</sup>, G. Giardina<sup>i,d</sup>, S. Giovannella<sup>h</sup>, E. Graziani<sup>t</sup>, F. Happacher<sup>h</sup>, L. Heijkskjöld<sup>v</sup>, B. Höistad<sup>v</sup>, M. Jacewicz<sup>v</sup>, T. Johansson<sup>v</sup>, K. Kacprzak<sup>g</sup>, D. Kamińska<sup>g</sup>, A. Kupsc<sup>v</sup>, J. Lee-Franzini<sup>h,u</sup>, F. Loddo<sup>b</sup>, S. Loffredo<sup>s,t</sup>, G. Mandaglio<sup>i,d,c</sup>, M. Martemianov<sup>j</sup>, M. Martini<sup>h,n</sup>, M. Mascolo<sup>q,r</sup>, R. Messi<sup>q,r</sup>, S. Miscetti<sup>h</sup>, G. Morello<sup>h</sup>, D. Moricciani<sup>r</sup>, P. Moskal<sup>g</sup>, F. Nguyen<sup>t,1</sup>, A. Palladino<sup>h</sup>, A. Passeri<sup>t</sup>, V. Patera<sup>m,h</sup>, I. Prado Longhi<sup>s,t</sup>, A. Ranieri<sup>b</sup>, P. Santangelo<sup>h</sup>, I. Sarra<sup>h</sup>, M. Schioppa<sup>e,f</sup>, B. Sciascia<sup>h</sup>, M. Silarski<sup>g</sup>, C. Taccini<sup>s,t</sup>, L. Tortora<sup>t</sup>, G. Venanzoni<sup>h</sup>, W. Wiślicki<sup>w</sup>, M. Wolke<sup>v</sup>, J. Zdebik<sup>g</sup>

<sup>a</sup> Dipartimento di Fisica dell'Università di Bari, Bari, Italy

<sup>b</sup> INFN Sezione di Bari, Bari, Italy

<sup>c</sup> Centro Siciliano di Fisica Nucleare e Struttura della Materia, Catania, Italy

<sup>d</sup> INFN Sezione di Catania, Catania, Italy

<sup>e</sup> Dipartimento di Fisica dell'Università della Calabria, Cosenza, Italy

<sup>f</sup> INFN Gruppo collegato di Cosenza, Cosenza, Italy

<sup>g</sup> Institute of Physics, Jagiellonian University, Cracow, Poland

<sup>h</sup> Laboratori Nazionali di Frascati dell'INFN, Frascati, Italy

<sup>i</sup> Dipartimento di Fisica e Scienze della Terra dell'Università di Messina, Messina, Italy

<sup>j</sup> Institute for Theoretical and Experimental Physics (ITEP), Moscow, Russia

<sup>k</sup> Dipartimento di Fisica dell'Università "Federico II", Napoli, Italy

<sup>l</sup> INFN Sezione di Napoli, Napoli, Italy

<sup>m</sup> Dipartimento di Scienze di Base ed Applicate per l'Ingegneria dell'Università "Sapienza", Roma, Italy

<sup>n</sup> Dipartimento di Scienze e Tecnologie applicate, Università "Guglielmo Marconi", Roma, Italy

<sup>o</sup> Dipartimento di Fisica dell'Università "Sapienza", Roma, Italy

<sup>p</sup> INFN Sezione di Roma, Roma, Italy

<sup>q</sup> Dipartimento di Fisica dell'Università "Tor Vergata", Roma, Italy

<sup>r</sup> INFN Sezione di Roma Tor Vergata, Roma, Italy

<sup>s</sup> Dipartimento di Matematica e Fisica dell'Università "Roma Tre", Roma, Italy

<sup>t</sup> INFN Sezione di Roma Tre, Roma, Italy

<sup>u</sup> Physics Department, State University of New York at Stony Brook, USA

<sup>v</sup> Department of Physics and Astronomy, Uppsala University, Uppsala, Sweden

<sup>w</sup> National Centre for Nuclear Research, Warsaw, Poland

\* Corresponding author at: INFN Sezione di Roma, Roma, Italy.

E-mail address: antonio.desantis@roma1.infn.it (A. De Santis).

URL: <http://www.lnf.infn.it/~adesanti> (A. De Santis).

<sup>1</sup> Present address: Laboratório de Instrumentação e Física Experimental de Partículas, Lisbon, Portugal.

## ARTICLE INFO

## Article history:

Received 24 December 2013  
 Accepted 13 January 2014  
 Available online 17 January 2014  
 Editor: L. Rolandi

## Keywords:

CPT symmetry  
 Lorentz symmetry  
 Neutral kaons  
 $\phi$ -Factory

## ABSTRACT

Neutral kaon pairs produced in  $\phi$  decays in anti-symmetric entangled state can be exploited to search for violation of CPT symmetry and Lorentz invariance. We present an analysis of the CP-violating process  $\phi \rightarrow K_S K_L \rightarrow \pi^+ \pi^- \pi^+ \pi^-$  based on  $1.7 \text{ fb}^{-1}$  of data collected by the KLOE experiment at the Frascati  $\phi$ -factory DAΦNE. The data are used to perform a measurement of the CPT-violating parameters  $\Delta a_\mu$  for neutral kaons in the context of the Standard Model Extension framework. The parameters measured in the reference frame of the fixed stars are:

$$\Delta a_0 = (-6.0 \pm 7.7_{\text{stat}} \pm 3.1_{\text{syst}}) \times 10^{-18} \text{ GeV},$$

$$\Delta a_X = (0.9 \pm 1.5_{\text{stat}} \pm 0.6_{\text{syst}}) \times 10^{-18} \text{ GeV},$$

$$\Delta a_Y = (-2.0 \pm 1.5_{\text{stat}} \pm 0.5_{\text{syst}}) \times 10^{-18} \text{ GeV},$$

$$\Delta a_Z = (3.1 \pm 1.7_{\text{stat}} \pm 0.5_{\text{syst}}) \times 10^{-18} \text{ GeV}.$$

These are presently the most precise measurements in the quark sector of the Standard Model Extension.

© 2014 The Authors. Published by Elsevier B.V. This is an open access article under the CC BY license (<http://creativecommons.org/licenses/by/3.0/>). Funded by SCOAP<sup>3</sup>.

## 1. Introduction

The CPT theorem [1] ensures invariance under the simultaneous transformation of charge conjugation (C), parity (P) and time reversal (T), in the context of local quantum field theories with Lorentz invariance and Hermiticity. On the other hand CPT violation in any unitary, local, point-particle quantum field theory entails Lorentz invariance violation, as proved in a theorem by Greenberg [2]. Even though Lorentz symmetry has been verified in many experiments, as also CPT invariance, it can be considered a sensitive probe for physics at the Planck scale, where natural mechanisms for such violations exist in quantum theories of gravity [3].

An attractive possibility to describe CPT and Lorentz violation effects in the low energy regime accessible to experiments consists of using an effective field theory, independent of the underlying mechanism generating CPT and Lorentz violation. This can be obtained by adding to the Standard Model action all possible scalar terms formed by contracting operators for simultaneous CPT and Lorentz violation with coefficients that control the size of the effects. The resulting effective field theory, the Standard Model Extension (SME) [4], appears to be compatible with the basic tenets of quantum field theory and retains the properties of gauge invariance and renormalizability. The SME is quite general and widely used in a broad class of experimental tests of CPT and Lorentz symmetry in several physics domains ranging from atomic physics to particle physics and to cosmology [5].

In the present Letter we present a test of CPT and Lorentz symmetry in the neutral kaon system within the SME framework. It has been performed by analyzing the  $\phi \rightarrow K_S K_L \rightarrow \pi^+ \pi^- \pi^+ \pi^-$  events collected by the KLOE experiment at the DAΦNE  $\phi$ -factory.

The physical neutral kaon states are expressed in terms of the flavor states as  $|K_{S,L}\rangle \propto (1 + \epsilon_{S,L})|K^0\rangle \pm (1 - \epsilon_{S,L})|\bar{K}^0\rangle$ , with  $\epsilon_{S,L} = \epsilon_K \pm \delta_K$  being the CP impurities ( $\epsilon_K$  and  $\delta_K$  are the usual T and CPT violation parameters). In SME CPT violation manifests to lowest order only in the mixing parameter  $\delta_K$  (i.e. vanishes at first order in the decay amplitudes), and exhibits a dependence on the 4-momentum of the kaon [6]:

$$\delta_K \approx i \sin \phi_{SW} e^{i\phi_{SW}} \gamma_K (\Delta a_0 - \vec{\beta}_K \cdot \Delta \vec{a}) / \Delta m, \quad (1)$$

where  $\gamma_K$  and  $\vec{\beta}_K$  are the kaon boost factor and velocity in the laboratory frame,  $\phi_{SW} = \arctan(2\Delta m / \Delta \Gamma)$  is the so-called *superweak* phase,  $\Delta m = m_L - m_S$ ,  $\Delta \Gamma = \Gamma_S - \Gamma_L$  are the mass and width differences for the neutral kaon mass eigenstates, and  $\Delta a_\mu$  are four CPT and Lorentz violating coefficients for the two valence quarks

in the kaon.<sup>2</sup> The natural choice of the reference frame to observe these parameters is the reference frame defined by fixed stars. Following Ref. [6] and choosing a three-dimensional basis  $(\hat{X}, \hat{Y}, \hat{Z})$  in this frame (with  $\hat{Z}$  parallel to Earth's rotation axis,  $\hat{X}$  expressed in terms of celestial equatorial coordinates with declination and right ascension  $0^\circ$ , while  $\hat{Y}$  with declination  $0^\circ$  and right ascension  $90^\circ$ ) and a basis  $(\hat{x}, \hat{y}, \hat{z})$  for the laboratory frame according to Fig. 1(left), (where  $\hat{z}$  is parallel to the beam axis with direction fixed by the positron beam and  $\hat{x}$  lies in the plane  $(\hat{z}, \hat{Z})$ ), the CPT violating parameter  $\delta_K$  is expressed as:

$$\begin{aligned} \delta_K(\vec{p}, t_s) = & \frac{i \sin \phi_{SW} e^{i\phi_{SW}}}{\Delta m} \gamma_K [\Delta a_0 \\ & + \beta_K \Delta a_Z (\cos \vartheta \cos \chi - \sin \vartheta \cos \varphi \sin \chi) \\ & - \beta_K \Delta a_X \sin \vartheta \sin \varphi \sin \Omega t_s \\ & + \beta_K \Delta a_Y (\cos \vartheta \sin \chi + \sin \vartheta \cos \varphi \cos \chi) \cos \Omega t_s \\ & + \beta_K \Delta a_Y (\cos \vartheta \sin \chi + \sin \vartheta \cos \varphi \cos \chi) \sin \Omega t_s \\ & + \beta_K \Delta a_Y \sin \vartheta \sin \varphi \cos \Omega t_s] \end{aligned} \quad (2)$$

where  $\vec{p}$  is the kaon momentum,  $t_s$  is the sidereal time,  $\Omega$  is the Earth's sidereal frequency,  $\cos \chi = \hat{z} \cdot \hat{Z}$ ;  $\vartheta$  and  $\varphi$  are the conventional polar and azimuthal angles of the kaon momentum in the laboratory frame.

The sensitivity to the four  $\Delta a_\mu$  parameters can be very different for fixed target and collider experiments, showing complementary features [6,7]. At a fixed target experiment the kaon momentum direction is fixed, while  $|\vec{p}|$  might vary within a certain interval. On the contrary, at a  $\phi$ -factory kaons are emitted in all directions with the characteristic  $p$ -wave angular distribution  $dN/d\Omega \propto \sin^2 \vartheta$ , while  $|\vec{p}|$  is almost fixed.<sup>3</sup> The analysis strategy used to measure the four  $\Delta a_\mu$  parameters exploits the entanglement of neutral kaons produced at DAΦNE [7]. In fact, at a  $\phi$ -factory, neutral kaons are produced in pairs in a coherent quantum state with the  $\phi$ -meson quantum numbers  $J^{PC} = 1^{--}$ :

$$\begin{aligned} |i\rangle = & \frac{1}{\sqrt{2}} (|K^0, \vec{p}_1\rangle |\bar{K}^0, \vec{p}_2\rangle - |\bar{K}^0, \vec{p}_1\rangle |K^0, \vec{p}_2\rangle) \\ = & \frac{\mathcal{N}}{\sqrt{2}} (|K_S, \vec{p}_1\rangle |K_L, \vec{p}_2\rangle - |K_L, \vec{p}_1\rangle |K_S, \vec{p}_2\rangle) \end{aligned} \quad (3)$$

<sup>2</sup>  $\Delta a_\mu$  parameters are associated with differences of terms in the SME of the form  $-a_\mu^q \bar{q} \gamma^\mu q$ , where  $q$  is a quark field of a specific flavor [6].

<sup>3</sup> At DAΦNE  $|\vec{p}|$  is not fixed because of a small  $\phi$  meson momentum  $\vec{p}_\phi$  in the laboratory frame ( $|\vec{p}_\phi| \simeq 15 \text{ MeV}$ ).

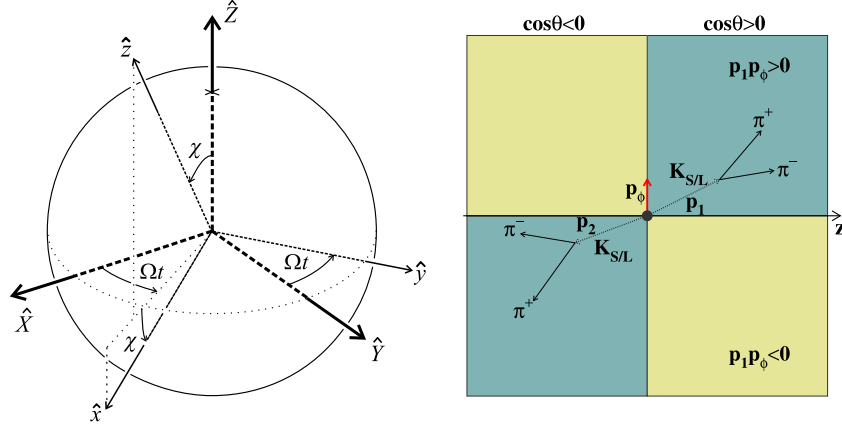


**Fig. 1.** Left: basis  $(\hat{x}, \hat{y}, \hat{z})$  for the lab frame, and basis  $(\hat{X}, \hat{Y}, \hat{Z})$  for the fixed stars frame. The laboratory frame precesses around the Earth's rotation axis  $\hat{Z}$  at the sidereal frequency  $\Omega$ . The angle between  $\hat{Z}$  and the positron beam direction  $\hat{z}$  defined in the laboratory frame of KLOE is  $\chi \simeq 113^\circ$  (picture taken from Ref. [6]). Right: sketch of the quadrant subdivisions as seen from a top view of the KLOE detector;  $\vec{p}_\phi$  is lying in the horizontal plane.

where  $\mathcal{N} = \sqrt{(1 + |\epsilon_S|^2)(1 + |\epsilon_L|^2)/(1 - \epsilon_S \epsilon_L)} \simeq 1$  is a normalization factor and  $\vec{p}_1, \vec{p}_2$  are the kaon momenta.

The observable quantity is the double differential decay rate of the state  $|i\rangle$  into decay products  $f_1$  and  $f_2$  at proper times  $\tau_1$  and  $\tau_2$ , respectively. After integration on  $(\tau_1 + \tau_2)$  at fixed time difference  $\Delta\tau = \tau_1 - \tau_2$ , the decay intensity can be written as follows [7]:

$$I_{f_1 f_2}(\Delta\tau) = C_{12} e^{-\Gamma|\Delta\tau|} [|\eta_1|^2 e^{-\frac{\Delta\Gamma}{2}\Delta\tau} + |\eta_2|^2 e^{-\frac{\Delta\Gamma}{2}\Delta\tau} - 2\Re(\eta_1 \eta_2^* e^{-i\Delta m \Delta\tau})] \quad (4)$$

with  $\Gamma = (\Gamma_S + \Gamma_L)/2$ ,

$$\eta_j \equiv |\eta_j| e^{i\phi_j} = \frac{\langle f_j | T | K_L \rangle}{\langle f_j | T | K_S \rangle},$$

$$C_{12} = \frac{|\mathcal{N}|^2}{2(\Gamma_S + \Gamma_L)} |\langle f_1 | T | K_S \rangle \langle f_2 | T | K_S \rangle|^2.$$

In particular when  $f_1 = f_2 = \pi^+ \pi^-$  ( $I_{f_1, f_2}(\Delta\tau) \equiv I_{\pm}(\Delta\tau)$ ) the corresponding  $\eta_j$  parameters can be slightly different for the two kaons due to the momentum dependence of the CPT violation effects arising from Eq. (2):

$$\begin{aligned} \eta_1 &\simeq \epsilon_K - \delta_K(\vec{p}_1, t_s), \\ \eta_2 &\simeq \epsilon_K - \delta_K(\vec{p}_2, t_s), \end{aligned} \quad (5)$$

with  $\vec{p}_2 = \vec{p}_\phi - \vec{p}_1$ . Higher order contributions to CP violation common to the two  $\eta_j$  coefficients have been neglected. Due to the presence of the fully destructive quantum interference at  $\Delta\tau = 0$ , the distribution  $I_{\pm}(\Delta\tau)$  is extremely sensitive to any deviation from unity of the ratio  $\eta_1/\eta_2$  in this interference region<sup>4</sup> (i.e.  $\Delta\tau \approx 0$ ). Therefore a suitable analysis of the decays  $\phi \rightarrow K_S K_L \rightarrow \pi^+ \pi^- \pi^+ \pi^-$  as a function of sidereal time and kaon momenta can provide a measurement of the four parameters  $\Delta a_\mu$ .

It is worth noting that the presence of the small momentum  $\vec{p}_\phi$  makes  $\gamma_1 \neq \gamma_2$  on an event-by-event basis, which is a necessary condition in order to have the  $I_{\pm}(\Delta\tau)$  distribution sensitive to the CPT violation effects induced by the  $\Delta a_0$  parameter.

The two kaons are identified by their emission in the forward ( $\cos\vartheta > 0$ ) or backward ( $\cos\vartheta < 0$ ) hemispheres, as shown in

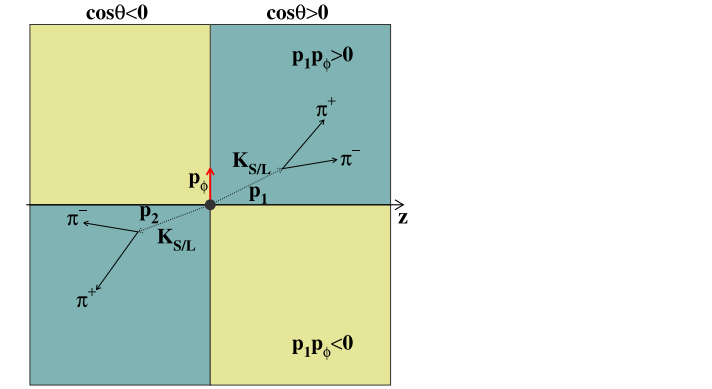


Fig. 1(right). The data sample is divided into two subsets in which the kaons going in the forward direction ( $\cos\vartheta > 0$ ) are emitted in a quadrant along with  $(\vec{p}_1 \cdot \vec{p}_\phi > 0)$  or opposite to  $(\vec{p}_1 \cdot \vec{p}_\phi < 0)$  the  $\phi$  momentum  $\vec{p}_\phi$ , thus having a higher (or lower) value of  $\gamma_1$  than the companion kaons emitted in the backward direction (see Fig. 1(right)). Moreover, the data are divided into four bins of sidereal time. Fitting simultaneously the corresponding eight  $I_{\pm}(\Delta\tau)$  distributions modulation effects induced by the CPT-violating parameter  $\delta_K$  in Eq. (2) as a function of sidereal time and kaon momentum can be observed.

The observable decay rate distribution as a function of  $\Delta\tau$  for these bins is:

$$S_{jh}(\Delta\tau) = \int_{\Delta t_{sj}} dt_s \rho(t_s) \int_{\Delta\Omega_h} d\varphi d\vartheta g(\vartheta) I_{\pm}(\Delta\tau). \quad (6)$$

The function  $\rho(t_s)$  is the sidereal time density of recorded events and has been derived from an independent data sample. Indices  $j = 1, 4$  and  $h = 1, 2$  are for the sidereal time and angular bin, respectively. The factor  $g(\vartheta)$  takes into account the kaon polar angle distribution in the  $\phi$  meson center of mass frame ( $\sin^3\vartheta$ ).

Starting from Eq. (6) the expected distribution is:

$$\begin{aligned} \tilde{S}_{jh}(\Delta\tau) &= (1 + f_{\text{regen}}(\Delta\tau)) \\ &\times \int d\Delta\tau' \varepsilon_{\text{tot}}(\Delta\tau') P_{\text{MC}}(\Delta\tau' - \Delta\tau) S_{j,h}(\Delta\tau') \end{aligned} \quad (7)$$

where  $f_{\text{regen}}(\Delta\tau)$  is a correction factor that takes into account the kaon regeneration on the beam pipe structures,  $\varepsilon_{\text{tot}}(\Delta\tau')$  is the total detection efficiency, and  $P_{\text{MC}}(\Delta\tau' - \Delta\tau)$  is the smearing matrix for the  $\Delta\tau$  resolution, both evaluated with the Monte Carlo (MC) simulation. The correction induced by kaon regeneration has been evaluated according to Ref. [8].

## 2. The KLOE experiment

The KLOE experiment operates at DAΦNE, the Frascati  $\phi$ -factory. DAΦNE is an  $e^+e^-$  collider working at a center of mass energy of  $\sim 1020$  MeV, the mass of the  $\phi$ -meson. Positron and electron beams collide at an angle of  $\pi - 25$  mrad, producing  $\phi$  mesons with non-zero momentum in the horizontal plane,  $|\vec{p}_\phi| \sim 15$  MeV in the KLOE reference frame.

The beam pipe at the interaction region of DAΦNE has a spherical shape, with a radius of 10 cm, and is made of an aluminum-beryllium alloy 500  $\mu\text{m}$  thick. A thin beryllium cylinder, 50  $\mu\text{m}$  thick and 4.4 cm radius, is inserted to ensure electrical continuity.

<sup>4</sup> Outside the interference region  $|\Delta\tau| \gg \tau_S$  the distribution  $I_{\pm}(\Delta\tau)$  is only sensitive to deviations from unity of the ratio  $|\eta_1/\eta_2|^2$ . In this case no CPT violation effect can be observed because  $\epsilon_K$  and  $\delta_K$  are expected to be  $90^\circ$  out of phase (i.e.  $\Re(\delta_K/\epsilon_K) \sim 0$ ).

The KLOE detector consists of a large cylindrical drift chamber (DC) surrounded by a lead-scintillating fiber electromagnetic calorimeter (EMC). A super-conducting coil around the EMC provides a 0.52 T axial field.

The DC [9] is 4 m in diameter and 3.3 m long and has 12,582 all-stereo cells properly arranged in 58 layers to ensure homogeneous detector response. Time and amplitude of signals from cells are read-out to measure hit positions and energy loss [10]. The chamber structure is made of carbon-fiber epoxy composite and the gas mixture used is 90% helium, 10% isobutane. These features maximize transparency to photons and reduce  $K_L \rightarrow K_S$  regeneration and multiple scattering. The position resolutions for single hits are  $\sigma_{r,\phi} \sim 150 \mu\text{m}$  and  $\sigma_z \sim 2 \text{ mm}$  in the transverse and longitudinal plane, respectively and are almost homogeneous in the active volume. The momentum resolution is  $\sigma(p_\perp)/p_\perp \sim 0.4\%$  for polar angles in the range  $40^\circ$ – $130^\circ$ .

The EMC [11] is divided into a barrel and two end-caps, and covers 98% of the solid angle. Signal amplitude and time of the modules are read-out at both ends by photo-multipliers for a total of 2440 cells arranged in five layers in depth. Cells close in time and space are grouped into calorimeter clusters. The cluster energy  $E_{\text{clu}}$  is the sum of its cell energies. The cluster time  $T_{\text{clu}}$  and position  $R_{\text{clu}}$  are energy-weighted averages. Energy and time resolutions are  $\sigma_E/E_{\text{clu}} = 5.7\%/\sqrt{E_{\text{clu}}} \text{ (GeV)}$  and  $\sigma_{T_{\text{clu}}} = (57 \text{ ps})/\sqrt{E_{\text{clu}}} \text{ (GeV)} \oplus 100 \text{ ps}$ , respectively.

During data taking DAΦNE beam conditions and detector calibrations are constantly monitored in order to guarantee the highest quality of the collected data.

### 3. Data analysis

A integrated luminosity of  $1.7 \text{ fb}^{-1}$  have been used in this analysis, corresponding to the KLOE data-set acquired during years 2004–2005. Two different MC samples have been used, with equivalent integrated luminosity of  $3.4 \text{ fb}^{-1}$  and  $17 \text{ fb}^{-1}$ , respectively. The former, containing all the  $\phi$ -meson decay channels, have been used for analysis optimization, while the latter, containing signal events only, have been used for efficiency and  $\Delta\tau$  resolution determination.

The data reduction starts with the topological identification of the candidate signal events: two decay vertices with only two tracks each. For each vertex the same kinematic criteria are used for sample selection:

- $|m_{\text{trk}} - m_K| < 5 \text{ MeV}$ , where  $m_{\text{trk}}$  is the invariant mass of the kaon reconstructed from the tracks assuming charged pion mass hypothesis:  $\vec{p}_{1,2} = \vec{p}_{\pi^+} + \vec{p}_{\pi^-}$  and  $E_{1,2} = E_{\pi^+} + E_{\pi^-}$ . Energy of the pions are defined as:  $E_\pi = \sqrt{m_\pi^2 + |\vec{p}_\pi|^2}$ ;
- $\sqrt{E_{\text{miss}}^2 + |\vec{p}_{\text{miss}}|^2} < 10 \text{ MeV}$ , where  $\vec{p}_{\text{miss}} = (\vec{p}_\phi - \vec{p}_{2,1}) - \vec{p}_{1,2}$  and  $E_{\text{miss}} = (E_\phi - E_{2,1}) - E_{1,2}$ ;
- $-50 \text{ MeV}^2 < m_{\text{miss}}^2 < 10 \text{ MeV}^2$ , where  $m_{\text{miss}}^2 = E_{\text{miss}}^2 - |\vec{p}_{\text{miss}}|^2$ ;
- $|p_{1,2}^* - p_0^*| < 10 \text{ MeV}$ , where  $p_{1,2}^*$  is the momentum of the kaon, as derived from tracks, in the  $\phi$ -meson reference frame, while  $p_0^* = \sqrt{s/4 - m_K^2}$  and  $\sqrt{s}$  is the center-of-mass energy as measured run-by-run with large angle Bhabha scattering events.

In the analysis the two kaons are ordered according to the value of the longitudinal momentum,  $p_z$ . To avoid the region where this order is diluted by resolution effects, events with  $p_{1,z} < 2 \text{ MeV}$  are rejected.

In the standard data reconstruction [13] the position of the kaon decay vertex is determined using a purely geometrical ap-

proach (i.e., without kinematical information) and each vertex is fit independently of the rest of the event. In order to improve the accuracy of decay time measurements a dedicated fit procedure has been developed for this analysis. The free parameters of the fit are the  $\phi$ -meson decay point coordinates ( $\vec{V}_\phi$ ) and the decay length for the two kaons ( $\lambda_{1,2}$ ). The two vertices are assumed to be of the form  $\vec{V}_{1,2} = \vec{V}_\phi + \lambda_{1,2}\hat{n}_{1,2}$ , where  $\hat{n}_{1,2} = \vec{p}_{1,2}/|\vec{p}_{1,2}|$  is the flight direction of the kaon. A global Likelihood function is built in order to take into account both vertices at the same time:

$$-2 \log \mathcal{L} = \sum_{i=1,2} \log P_i(\vec{V}_i(\text{rec}) - \vec{V}_i(\text{fit})) + \log P_\phi(\vec{V}_\phi(\text{rec}) - \vec{V}_\phi(\text{fit})),$$

where  $P_j(P_\phi)$  are the probability density function for displacements with respect to the reconstructed positions as derived from MC. Events with  $-2 \log \mathcal{L} > 30$  or with pulls on decay length  $|\lambda_j(\text{rec}) - \lambda_j(\text{fit})|/\sigma_j(\text{fit}) > 10$  are rejected.

The  $\Delta\tau$  resolution is strongly correlated, as expected, with the opening angle of the pion tracks ( $\vartheta_\pm$ ), and deteriorates at large values of  $\vartheta_\pm$ . A cut to eliminate large opening angles values has been applied and events with  $\cos \vartheta_\pm < -0.975$  are rejected. The result is shown in Fig. 2(left). The core width of  $\Delta\tau$  resolution after all selection is  $\sim 0.6\tau_5$  as estimated by fitting the MC simulation distribution with the superposition of three Gaussian functions. The agreement with experimental data has been verified by comparing the kinematic fit pull distributions on decay length between experimental data and MC simulation.

The main background source is the kaon regeneration on the spherical beam pipe. In order to reduce this contribution the present analysis is restricted only to events with both  $K_S$  and  $K_L$  decaying inside the beam pipe. This geometrical requirement translates in maximal absolute value for  $\Delta\tau$  of  $12\tau_5$ . In this case kaon regeneration occurs only in the thin beryllium cylinder.

The residual background contamination in the  $\Delta\tau$  range  $[-12; 12]\tau_5$ , as estimated from MC simulation, is 2% from regeneration on the beryllium cylindrical foil and 0.5%  $e^+e^- \rightarrow \pi^+\pi^-\pi^+\pi^- (4\pi)$  direct production as estimated from a dedicated data analysis. The latter is concentrated around  $\Delta\tau \simeq 0$  while the former will be treated as a multiplicative correction applied to the fitting function as described in Eq. (7). The  $4\pi$  contribution is estimated to be  $54 \pm 5$  events, according to Ref. [8].

For the purpose of our measurement, precise knowledge of the total detection efficiency value ( $\varepsilon_{\text{tot}}$ ) is not required; it is however important to keep under control its dependence on  $\Delta\tau$ , shown in Fig. 2(right). The mean value is 25% for  $\Delta\tau$  ranging in  $[-12; 12]\tau_5$  with a consistent drop for  $\Delta\tau \sim 0$ . This is due to two concurrent effects: increasing extrapolation length for tracks coming from decays very close to the beam interaction point and wrong association of tracks to the kaon decay vertices.<sup>5</sup> The efficiency  $\varepsilon_{\text{tot}}$  can be divided into three main components, related to the trigger, to the reconstruction procedure and to the effect of the selection criteria:

$$\varepsilon_{\text{tot}} = \varepsilon_{\text{trig}} \varepsilon_{\text{reco}} \varepsilon_{\text{cuts}}.$$

The last contribution is derived from MC simulation while for trigger and reconstruction efficiencies, corrections obtained from real data are used. To this aim a high purity, independent control sample of  $K_S \rightarrow \pi^+\pi^-$  and  $K_L \rightarrow \pi\mu\nu$  has been selected with particles in the same momentum range as for the signal.

<sup>5</sup> When the two vertices are so close in space ( $\Delta\tau \sim 1\tau_5 \Rightarrow \Delta\lambda_V \sim 6 \text{ mm}$ ) it is possible to wrongly associate tracks to vertex by exchanging two of them. These vertices are then rejected because of the kinematical requirements.

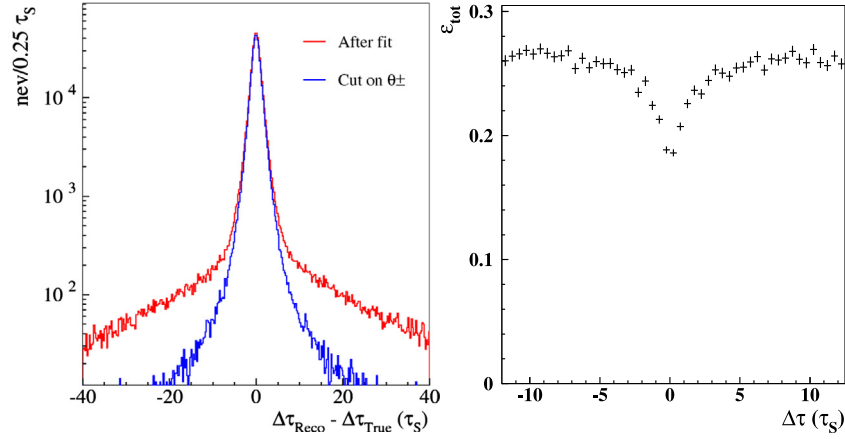


**Fig. 2.** Left: resolution on  $\Delta\tau$  variable evaluated from MC simulation as the difference between true values and data-like reconstructed values. The effect of the cut on the opening angle between tracks is shown. Right: total detection efficiency as a function of true  $\Delta\tau$  as observed from MC simulation. The dip around  $\Delta\tau \sim 0$  is discussed in the text.

**Table 1**

Fit results. Errors include all source of the statistical fluctuations. The fit  $\chi^2/N_{\text{Dof}}$  is 211.7/187 corresponding to a probability of 10%. The table contains the correlation coefficient matrix between the parameters.

Fit output ( $10^{-18}$ GeV units)	Correlation matrix			
$\Delta a_0 = -6.0 \pm 7.7$	1.000	0.304	-0.187	0.483
$\Delta a_X = 0.9 \pm 1.5$	0.304	1.000	-0.045	0.069
$\Delta a_Y = -2.0 \pm 1.5$	-0.187	-0.045	1.000	-0.104
$\Delta a_Z = 3.1 \pm 1.7$	0.483	0.069	-0.104	1.000

The purity of the control sample is 95%, the background being dominated by  $K_{e3}$  decay. The efficiency correction has been evaluated as the ratio between data and MC distributions of  $I_{K_{\mu 3\pm}}(\Delta\tau)$ . The decay time ordering criterion is the same used in the main analysis.

Experimental data distributions have been analyzed for different intervals of sidereal time and kaon emission angle using the function in Eq. (7). The  $\Delta\tau$  range is  $\Delta\tau \in [-12; 12]\tau_S$  with  $1\tau_S$  bin width, while sidereal time has 4 bins, 6 hours each, and two angular bins have been used:  $\vec{p}_1 \cdot \vec{p}_\phi \geq 0$  resulting in a total of 192 experimental points simultaneously fit. The fit  $\chi^2/N_{\text{Dof}}$  is 211.7/187 corresponding to a probability of 10%, numerical values of the fit are reported in Table 1 and the experimental data distributions are shown in Fig. 3.

Systematic effects are listed in Table 2. The full analysis chain has been repeated several times varying all the cuts values according to the MC resolution ( $\sigma_{\text{MC}}$ ) of the selection variables. Positive and negative variations ( $\pm\sigma_{\text{MC}}$ ) have been considered. The results of the fits are stable and the RMS of the distribution of obtained results is taken as systematic uncertainty.

The accuracy on the determination of the  $\Delta a_0$  parameter strongly depends on the stability of the observed  $I_{\pm}(\Delta\tau)$  distribution for  $|\Delta\tau| > 5\tau_S$ . For this reason the fit range has been varied of  $\pm 1\tau_S$  around the reference value enlarging or reducing the  $\Delta\tau$  range. Correspondingly the event yield varies of  $\sim 10\%$  and the RMS of the fit results has been chosen as the related systematic error. The largest effect, as expected, has been observed on  $\Delta a_0$ .

The  $4\pi$  background events is concentrated in the two bins around  $\Delta\tau \sim 0$ , resulting in a bin-by-bin contribution of  $\sim 3$  events, while the amount of observed data events in the same bins is around  $\sim 10$  events. Being the amount of subtracted events similar to the statistical uncertainty of the observed data the systematic effect of the subtraction has been obtained as the difference between results with and without subtraction.

The effect of the orientation of the KLOE reference frame with respect to the terrestrial coordinate system has been taken into

**Table 2**

Summary of the systematic uncertainty in  $10^{-18}$  GeV units.

	Analysis cut	$\Delta\tau$ range	$4\pi$ subtr.	Ref. frame	Total
$\Delta a_0$	1.1	2.4	1.3	1.0	3.1
$\Delta a_X$	0.3	0.3	0.4	0.2	0.6
$\Delta a_Y$	0.2	0.3	0.2	0.2	0.5
$\Delta a_Z$	0.2	0.2	0.4	0.4	0.6

account in the fit function. The measurement of the relative alignment between our reference frame with respect to the geographical frame has been performed with a compass and the effect of displacement between magnetic and true North pole has been taken into account and corrected for. The angle between the laboratory  $\hat{z}$  axis and the North direction is  $(130 \pm 2)^\circ$  on the local tangent plane. The fit function has been evaluated with angle variations up to  $10^\circ$  showing stable results. The RMS of the results has been taken as systematic uncertainty.

The kaon regeneration correction in Eq. (7) has been varied according to its relative uncertainty ( $\sim 35\%$ ). The corresponding results fluctuation is negligible with respect to the other systematic uncertainty.

The effect of mismatch in  $\Delta\tau$  resolution between experimental data and MC simulation has been found negligible inside the maximum allowable error of 5% on  $\Delta\tau$  resolution width.

The final systematics uncertainty is the sum in quadrature of all the discussed effects and is reported in the last column of Table 2. In all cases the total systematic uncertainty ranges between 30% and 40% of the corresponding statistical uncertainty.

## 4. Results and conclusions

The results for the  $\Delta a_\mu$  parameters are:

$$\begin{aligned} \Delta a_0 &= (-6.0 \pm 7.7_{\text{stat}} \pm 3.1_{\text{syst}}) \times 10^{-18} \text{ GeV}, \\ \Delta a_X &= (0.9 \pm 1.5_{\text{stat}} \pm 0.6_{\text{syst}}) \times 10^{-18} \text{ GeV}, \\ \Delta a_Y &= (-2.0 \pm 1.5_{\text{stat}} \pm 0.5_{\text{syst}}) \times 10^{-18} \text{ GeV}, \\ \Delta a_Z &= (3.1 \pm 1.7_{\text{stat}} \pm 0.5_{\text{syst}}) \times 10^{-18} \text{ GeV}. \end{aligned}$$

The systematic uncertainty is smaller than the corresponding statistical error implying that the main limitation of the present measurement is the available statistics. To this respect the continuation of the KLOE physics program in the framework of the KLOE-2 experiment [12] at upgraded DAΦNE machine [14] is important to further improve the results.

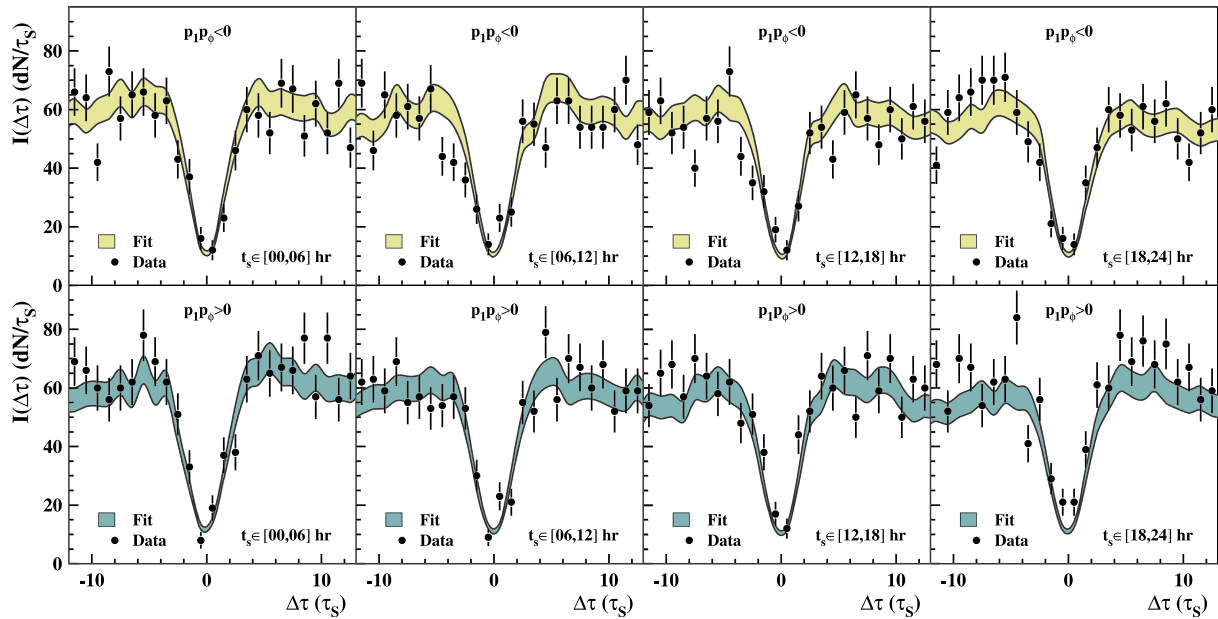


**Fig. 3.** Fit results: the top and bottom plots refer to the two angular selections. Black points are for experimental data while colored bands are the fit output. The error bars on experimental data are purely statistical, while the band represents the contribution to the uncertainty due to MC simulation statistics and efficiency correction.

The present result is the first complete measurement of all  $\Delta a_\mu$  parameters in the kaon sector.<sup>6</sup> The order of magnitude of the results is approaching the interesting region defined by  $m_R^2/\mathcal{M}_{\text{Planck}} \sim 2 \times 10^{-20}$  GeV in the assumption that the SME phenomenology of CPT and Lorentz invariance breaking is related to some underlying quantum gravity effects.

These results can be compared to similar ones for the corresponding  $\Delta a_\mu$  parameters for the B and D neutral meson systems [16,17] which have a precision of  $\mathcal{O}(10^{-13})$  GeV.

### Acknowledgements

We warmly thank our former KLOE colleagues for the access to the data collected during the KLOE data taking campaign. We thank the DAΦNE team for their efforts in maintaining low background running conditions and their collaboration during all data taking. We want to thank our technical staff: G.F. Fortugno and F. Sborzacchi for their dedication in ensuring efficient operation of the KLOE computing facilities; M. Anelli for his continuous attention to the gas system and detector safety; A. Balla, M. Gatta, G. Corradi and G. Papalino for electronics maintenance; M. Santoni, G. Paoluzzi and R. Rosellini for general detector support; C. Piscitelli for his help during major maintenance periods. We acknowledge the support of the European Community – Research Infrastructure Integrating Activity ‘Study of Strongly Interacting Matter’ (acronym Hadron-Physics2, Grant Agreement No. 227431) under the Seventh Framework Programme of EU. This work was supported also in part by the EU Integrated Infrastructure Initiative Hadron Physics Project under contract number RII3-CT-2004-506078; by the European Commission under the 7th Framework Programme through the ‘Research Infrastructures’ action of the ‘Capacities’ Programme, Call: FP7-INFRASTRUCTURES-2008-1, Grant Agreement No. 283286; by the Polish National Science Centre through the Grants Nos. 0469/B/H03/2009/37, 0309/B/H03/2011/40, DEC-2011/03/N/ST2/

02641, 2011/01/D/ST2/00748, 2011/03/N/ST2/02652, 2011/03/N/ST2/02641, 2013/08/M/ST2/00323, and by the Foundation for Polish Science through the MPD programme and the project HOMING PLUS BIS/2011-4/3.

### References

- [1] G. Lueders, *Ann. Phys.* 2 (1957) 1, reprinted in *Ann. Phys.* 281 (2000) 1004; W. Pauli, Exclusion principle, Lorentz group and reflexion of space-time and charge, in: W. Pauli (Ed.), *Niels Bohr and the Development of Physics*, Pergamon, London, 1955, p. 30; J.S. Bell, *Proc. R. Soc. Lond. Ser. A, Math. Phys. Sci.* 231 (1955) 479; R. Jost, *Helv. Phys. Acta* 30 (1957) 409.
- [2] O.W. Greenberg, *Phys. Rev. Lett.* 89 (2002) 231602.
- [3] V.A. Kostelecký, S. Samuel, *Phys. Rev. D* 39 (1989) 683; V.A. Kostelecký, R. Potting, *Nucl. Phys. B* 359 (1991) 545.
- [4] D. Colladay, V.A. Kostelecký, *Phys. Rev. D* 55 (1997) 6760; D. Colladay, V.A. Kostelecký, *Phys. Rev. D* 58 (1998) 116002; V.A. Kostelecký, R. Potting, *Phys. Rev. D* 51 (1995) 3923.
- [5] V.A. Kostelecký, N. Russell, *Rev. Mod. Phys.* 83 (2011) 11, updates on arXiv:0801.0287 [hep-ph].
- [6] V.A. Kostelecký, *Phys. Rev. Lett.* 80 (1998) 1818; V.A. Kostelecký, *Phys. Rev. D* 61 (1999) 016002; V.A. Kostelecký, *Phys. Rev. D* 64 (2001) 076001.
- [7] A. Di Domenico (Ed.), *Handbook on Neutral Kaon Interferometry at a  $\phi$ -Factory*, Frascati Phys. Ser., vol. 43, 2007.
- [8] F. Ambrosino, et al., KLOE Collaboration, *Phys. Lett. B* 642 (2006) 315.
- [9] M. Adinolfi, et al., *Nucl. Instrum. Methods Phys. Res., Sect. A, Accel. Spectrom. Detect. Assoc. Equip.* 488 (2002) 51.
- [10] A. Balla, M. Beretta, P. Branchini, P. Ciambone, G. Corradi, E. De Lucia, P. De Simone, G. Felici, et al., *Nucl. Instrum. Methods Phys. Res., Sect. A, Accel. Spectrom. Detect. Assoc. Equip.* 562 (2006) 141.
- [11] M. Adinolfi, et al., *Nucl. Instrum. Methods Phys. Res., Sect. A, Accel. Spectrom. Detect. Assoc. Equip.* 482 (2002) 363.
- [12] G. Amelino-Camelia, et al., *Eur. Phys. J. C* 68 (2010) 619.
- [13] F. Ambrosino, et al., KLOE Collaboration, *Nucl. Instrum. Methods Phys. Res., Sect. A, Accel. Spectrom. Detect. Assoc. Equip.* 534 (2004) 403.
- [14] M. Zobov, D. Alesini, M.E. Biagini, C. Biscari, A. Bocci, M. Boscolo, F. Bossi, B. Buonomo, et al., *Phys. Rev. Lett.* 104 (2010) 174801.
- [15] H. Nguyen, CPT results from KTeV, arXiv:hep-ex/0112046.
- [16] B. Aubert, et al., BaBar Collaboration, *Phys. Rev. Lett.* 100 (2008) 131802.
- [17] J.M. Link, et al., FOCUS Collaboration, *Phys. Lett. B* 556 (2003) 7.

<sup>6</sup> Preliminary results from KTeV collaboration in this sector can be found in the Ref. [15].